Chapter

Free Convection in a MHD Open Cavity with a Linearly Heated Wall Using LBM

Raoudha Chaabane

Abstract

This chapter examines the magneto-hydrodynamic (MHD) free convection in a square enclosure filled with liquid gallium subjected to a [transverse magnetic field] in-plane magnetic field. First, the side vertical walls of the cavity have spatially varying linearly temperature distributions. The bottom wall is uniformly heated and the upper wall is adiabatic. The second configuration is an open enclosure heated linearly from the left wall. Lattice Boltzmann method (LBM) is applied in order to solve the coupled equations of flow and temperature fields. This study has been carried out for Ra of 10^5. The results show that the heat transfer rate decreases with an increase of the Ha number which is a widely solicited result in different engineering applications. Streamlines, isotherm counters and Nu numbers are displayed and discussed. A good stability is observed for all studied cases employing an in-house code. The obtained results show that the free-convection heat transfer in the open MHD enclosure is enhanced and it is greater to that of a uniformly heated wall.

Keywords: MHD, open cavity, free convection, LBM, heat transfer

1. Introduction

Free convection in open cavities is an important phenomenon in engineering systems because of this it have received a considerable attention due to their applications in various industries of high-performance insulation for buildings, injection molding chemical catalytic reactors, packed sphere beds, grain storage, float glass production, air-conditioning in rooms, cooling of electronic devices, and geophysical problems. Extensive research studies using various numerical simulations were conducted into free convection of open enclosures [1–5]. The latter works have acquired a basic understanding of free convection flows and heat transfer characteristics in an open enclosure with non-conducting fluid. However, in most studies, one vertical wall of the enclosure is cooled and another one heated while the remaining top and bottom walls are well insulated. Recently, MHD free convection flows have attracted attention since can be are encountered in numerous problems with industrial and technological interest, covering a wide range of basic sciences such as nuclear engineering, fire research, crystal growth, astrophysics and metallurgy [6]. Besides, the process of manufacturing materials in industrial problems and microelectronic heat transfer devices involves an electrically conducting fluid

subjected to magnetic field. In this case the fluid experiences a Lorentz force reducing the flow velocities which affects the heat transfer rate [7, 8]. In MHD free convection flows, the balance is achieved by inertial, viscous, electromagnetic and buoyancy forces, rendering the solution more complicated. Other useful research works had been conducted to simulate the MHD free convection under different conditions [9–18]. Kahveci and Oztuna [19] investigated MHD free convection flow and heat transfer in a laterally heated partitioned enclosure. They showed that the horizontal magnetic field is more effective in damping convection than the vertical one. Furthermore, Kefayati et al. [20] investigated the effect of Ra number on free convection MHD in an open cavity. Nonetheless several investigations in MHD free convection inside open enclosure with linearly heated wall have been carried out. In addition to conventional free convection in enclosures with uniform thermic boundaries, recent attention has been intensively focused on the cases with mixed boundary conditions on the walls of an open cavity [21–24].

On the other hand, the Lattice Boltzmann Method (LBM) is a new method for simulating fluid flow and modeling physics in fluids. It has been applied extensively within the last decade. Based on kinetic theory for simulating fluid flows and modeling the physics in fluids [25–32], it becomes a powerful, effective and easy numerical method, for simulation of complex flow problems with different boundary conditions [33, 34].

In comparison with the conventional CFD methods, the LBM is based on the microscopic models, mesoscopic kinetic equations. The macroscopic dynamics of a fluid is the result of collective behavior of many microscopic particles in the system. The LBM has been proved to recover the Navier-Stokes equation by using the Chapman-Enskog expansion. The major advantage of this method is its explicit feature of the governing equation, easy for parallel computation and easy for implementation of irregular boundary conditions. To our best knowledge, no previous study on effects of linearly heated wall on free convection in an open MHD cavity with the LBM had already been studied so far. The main aim of this chapter is to study effects of linearly heated wall on flow field and temperature distribution in an open MHD cavity filled with liquid gallium and also to highlight the ability of the LBM for solving problems with various complex boundary conditions. The effects of Ra number on streamlines, isotherms and the Nusselt number are investigated.

2. Mathematical formulation

2.1 Problem statement

The considered model is shown in **Figure 1**. It displays a two-dimensional open cavity with side length of H. At first case the left vertical is maintained at high temperature (T_H). Whereas at the second case, the vertical left wall is linearly heated. An external cold air enters into the enclosure from the east opening boundary, while the fluid is correlated with open boundary at constant temperature (T_C). The horizontal walls are insulated and impermeable to mass transfer. The bottom wall is at high temperature TH and the top one is adiabatic. The open cavity is filled with liquid gallium with Pr number of 0.025. The gravitational acceleration acts downward. The uniform external magnetic field with a constant magnitude B_0 is applied in the x-direction (transverse field). It is assumed that the induced magnetic field produced by the motion of an electrically conducting fluid is negligible compared to the applied magnetic field. Thermo-physical properties of the fluid are assumed to be constant, and the density variation in the buoyancy force term is handled by the Boussinesq approximation. The flow is two-dimensional, laminar

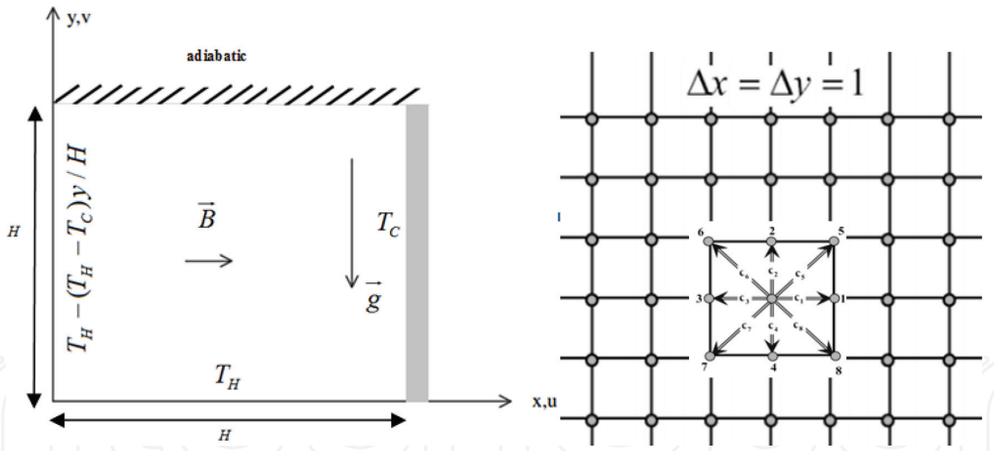

Figure 1.
Geometry of the present study with imposed boundary conditions and standard D_2Q_9 velocity mode.

and incompressible; in addition, it is assumed that the viscous dissipation and Joule heating are neglected.

2.2 Brief introduction to LBM

A scheme of the standard D2Q9 (**Figure 1**) for flow and for temperature, LBM method are used in this work [33–34] hence only brief discussion will be given in the following paragraphs, for completeness. Therefore, classic governing equations for MHD free convection are written in terms of the macroscopic variable depending on position x, y as:

Continuity equation

$$\frac{\partial u}{\partial x}+\frac{\partial v}{\partial y}=0 \tag{1}$$

Momentum equations

$$\rho\left(u\frac{\partial u}{\partial x}+v\frac{\partial u}{\partial y}\right)=-\frac{\partial p}{\partial x}+\mu\left(\frac{\partial^2 u}{\partial x^2}+\frac{\partial^2 u}{\partial y^2}\right)+F_x \tag{2}$$

$$\rho\left(u\frac{\partial v}{\partial x}+v\frac{\partial v}{\partial y}\right)=-\frac{\partial p}{\partial y}+\mu\left(\frac{\partial^2 v}{\partial x^2}+\frac{\partial^2 v}{\partial y^2}\right)+F_y \tag{3}$$

Energy equation

$$u\frac{\partial T}{\partial x}+v\frac{\partial T}{\partial y}=\alpha\left(\frac{\partial^2 T}{\partial x^2}+\frac{\partial^2 T}{\partial y^2}\right) \tag{4}$$

Where $\nu=\mu/\rho$ is the kinematic viscosity, F_x and F_y are the body forces at horizontal and vertical directions respectively and they are defined as follows [25]:

$$F_x=R\left(v\sin\gamma\cos\gamma-u\sin^2\gamma\right) \tag{5}$$

$$F_y=R\left(u\sin\gamma\cos\gamma-v\cos^2\gamma\right)+\rho g\beta(T-T_m) \tag{6}$$

Where the Ha number is defined as

$$Ha=LB_x\sqrt{\sigma/\mu} \tag{7}$$

In the LBM the total force is:

$$F = F_x + F_y \tag{8}$$

$$F_x = 3w_k\rho\left[R(v\sin\gamma\cos\gamma) - u\sin^2\gamma)\right] \tag{9}$$

$$F_y = 3w_k\rho\left[g_y\beta(T - T_m) + R(u\sin\gamma\cos\gamma) - v\cos^2\gamma\right] \tag{10}$$

Where $R = \mu Ha^2$ and γ is the direction of the magnetic field.

The functional density, velocity and temperature in the mesoscopic approach are:

$$\rho(\mathbf{r},t) = \sum_k f_k(\mathbf{r},t) \tag{11}$$

$$\mathbf{u}(\mathbf{r},t) = \sum_k \mathbf{c}_k f_k(\mathbf{r},t)/\rho(\mathbf{r},t) \tag{12}$$

$$T = \sum_k g_k(\mathbf{r},t) \tag{13}$$

2.3 Method of solution

To ensure that the <code simulates an approximated incompressible regime>, the characteristic velocity of the flow ($V = \sqrt{g\beta_T H(T_w - T_\infty)}$) at the free convection regime must be compared with the fluid speed of sound c_s. In the present study, the characteristic velocity is selected as 0.1 of sound speed. By fixing Ra number $Ra = \beta g_y H^3 \mathrm{Pr}(T_H - T_C)/\nu^2$, Pr number $\mathrm{Pr} = \alpha\nu$ and Mach number ($Ma = u/c$), the kinematic viscosity $\nu = Ma\,Ha\,c_s\sqrt{\mathrm{Pr}/Ra}$ and thermal diffusivity α are deduced. Nusselt number Nu is one of the most important dimensionless parameters in describing the convective and thermic heat transport. For the example, the local Nusselt number and the average value at the left side wall are calculated as;

$$Nu_y = -\frac{H}{T_H - T_C}\left.\frac{\partial T}{\partial x}\right|_{x=0} \tag{14}$$

$$Nu_{av} = \frac{1}{H}\int_0^H Nu_y dy \tag{15}$$

2.4 Algorithm of the numerical procedure

In this section, we present the steps that must be executed for the numerical implementation:

1. Input constant parameters.

2. Calculate the relaxation times.

3. Initialize the temperature, and velocity fields for the entire computational domain and the equilibrium distribution functions.

4. Calculate the current distribution function for propagation of temperature and velocity.

5. Propagate all current distribution functions to the neighbor lattices in all directions.

6. Impose the boundary conditions.

7. Calculate the current temperature and velocity field for the entire computational domain and the current equilibrium distribution functions using the current temperature and velocity fields.

8. The error convergence is checked, if the error does not satisfies the convergence criterion, go to step 4.

3. Results and discussion

For all further numerical cases, both for flow and temperature fields, the computations are based on an iterative LBM used for obtaining the numerical simulations. In order to validate the numerical code, the pure free convection, in a square open cavity with insulated horizontal walls filled with air was solved, and the results were compared with the numerical ones reported by reference [20]. The present findings are obtained with an extended computational domain. In **Figure 2**, we depict the comparison of the streamlines and isotherms of the present study with the prediction of [20]. Obtained results demonstrate that a good agreement was achieved. Also, in **Figure 3**, a comparison of isotherms and streamlines demonstrate a good agreement with previous work [7] where the considered matter is MHD free convection in a closed cavity with linearly heated west wall which is filled with liquid gallium (Pr = 0.025) and Ha = 50. The present chapter extend the study to deal with free convection in MHD open cavity with constant or linearly heated west wall which is filled with liquid gallium with Pr = 0.025 and Ha = 50 for Ra = 10^5.

The heat transfer rate is highlighted within the local and average Nusselt number in the case of linearly heated side walls. **Figure 4b** illustrates the variation of the local Nusselt number at the bottom wall of the cavity Nu_b with the horizontal normalized distance x/X for the case of linearly heated side walls with Ha = 50, Pr = 0.025 and Ra = 10^5. The Nusselt local value at the bottom is equal to unity at the

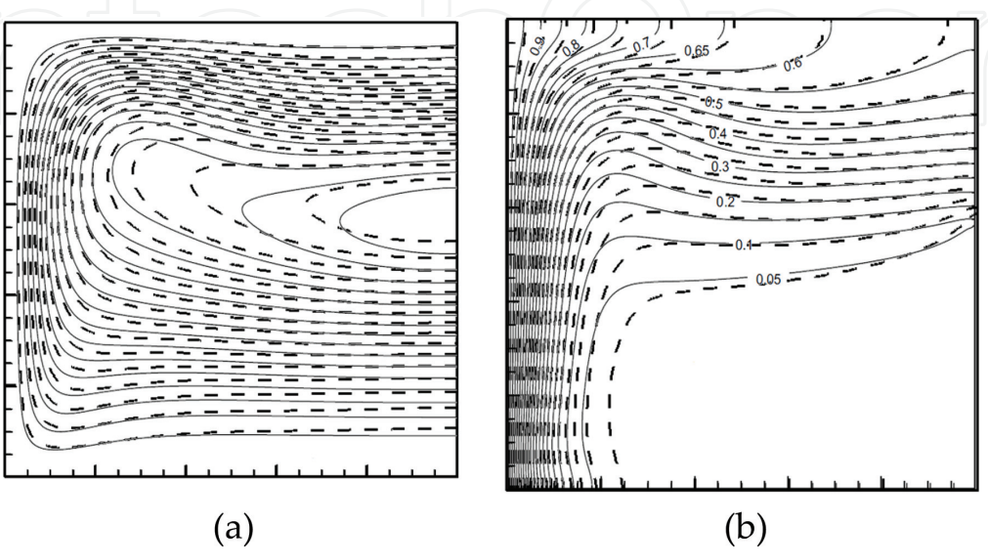

Figure 2.
Comparison of the steady state streamlines (a) and isotherms (b) at Pr = 0.71 for Ha = 0 and Ra = 10^5 between [20] (continuous lines) and the present work (dashed lines).

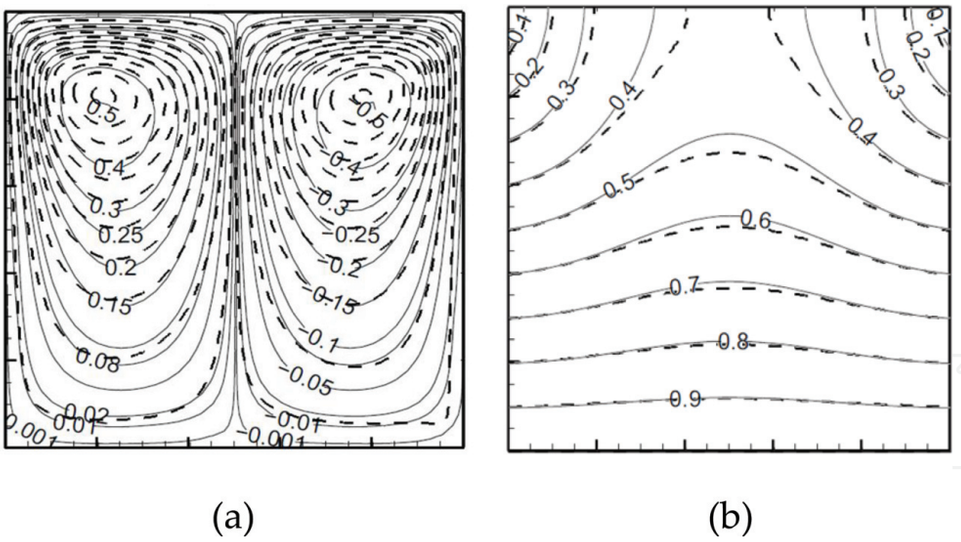

Figure 3.
Of the steady state fluid velocity streamlines (a) and isotherms (b) of linearly heated side walls MHD cavity for Ha = 50, Pr = 0.025 and Ra = 10^5 between [7] (continuous lines) and the present work (dashed lines). Frame ranges [−0.001, 0.5] (a), frame ranges [0, 1] (b).

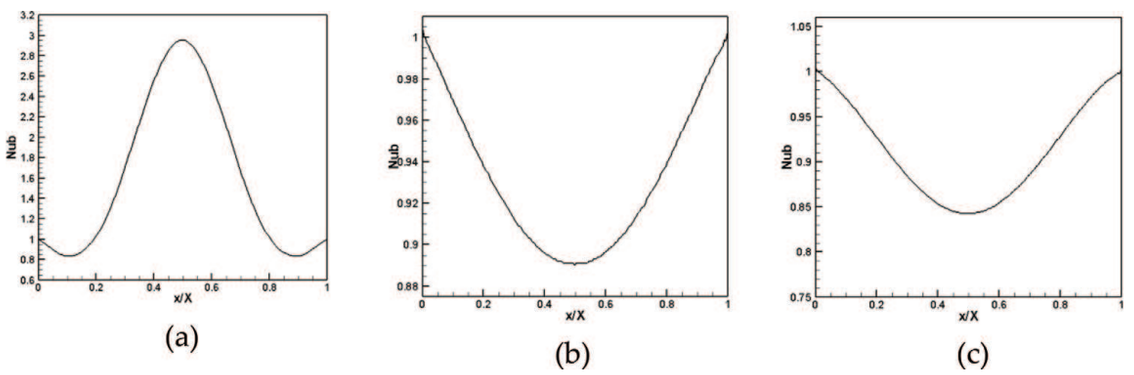

Figure 4.
Variation of bottom Nusselt number with distance at bottom wall in the case of linearly heated side walls (Pr = 0.025 and Ra = 10^5) for different Ha numbers. (a) Ha = 0, (b) Ha = 50 and (c) Ha = 150.

left (x/X = 0) and right (x/X = 1). This is an expected result due to the linearly heated side walls. The latter is associated with the symmetry in the thermic boundary conditions of the side walls of the cavity. **Figure 4a–c** shows clearly that the local Nusselt number at the bottom wall Nu_b exhibits an oscillatory behavior with the horizontal distance x/X and that it is exactly symmetric about the centerline of the bottom wall. The Variation of local Nusselt number with distance at bottom wall in the case of linearly heated side walls (Pr = 0.025 and Ra = 10^5) is depicted for different Ha numbers. **Figure 5b** depicts the variation of the local Nusselt number at the linearly heated side walls of the cavity Nu sides with the vertical distance y/Y for Ha = 50 while **Figure 5a** depicts the variation of the local Nusselt number at the linearly heated side walls of the cavity Nu sides with the vertical distance y/Y for Ha = 0. In general, the values of Nu sides increase as the vertical distance y/Y increases reaching maximum at y/Y = 1. Also, for Ha = 0, the distributions of Nu sides along the vertical distance y/Y oscillate close to lower end of the vertical side wall and continues with an increasing trend in its upper end. This behavior is believed to be related the feature represented by two pairs of symmetric cells with clockwise and counter-clockwise rotations [7].

Figures 6 and 7 display steady-state contour maps for the isotherms and the streamlines contours at various Ha numbers (0, 50 and 100) for Pr = 0.025 and

DOI: http://dx.doi.org/10.5772/intechopen.81177

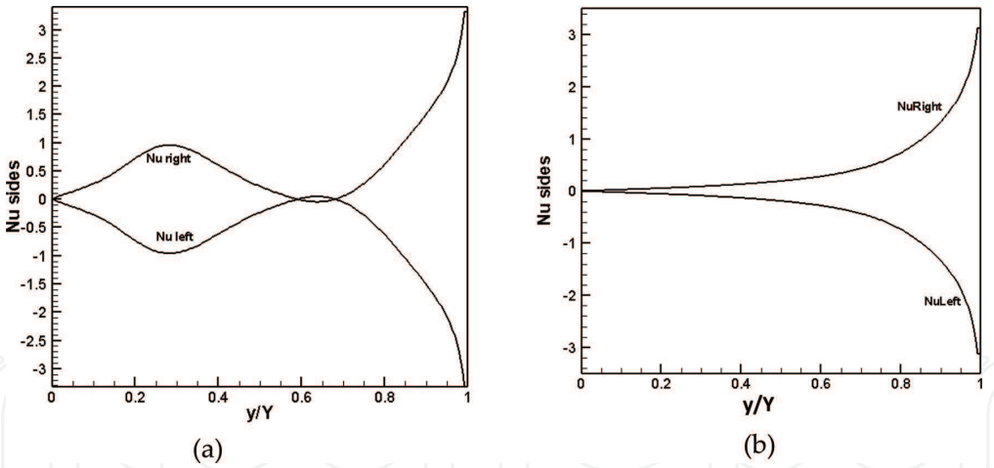

Figure 5.
Variation of local Nusselt number with distance at side wall for linearly heated side walls (Pr = 0.025 and Ra = 10^5). (a) Ha = 0 and (b) Ha = 50.

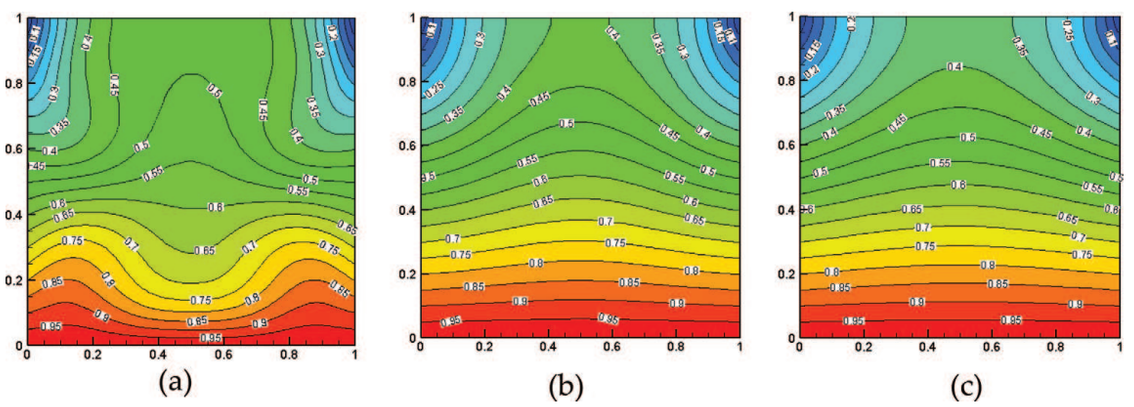

Figure 6.
Comparison of the steady state isotherms at Ra =10^5 and Pr = 0.025 for different Ha numbers in the case of linearly heated side walls. (a) Ha = 0 (b) Ha = 50 and (c) Ha = 100.

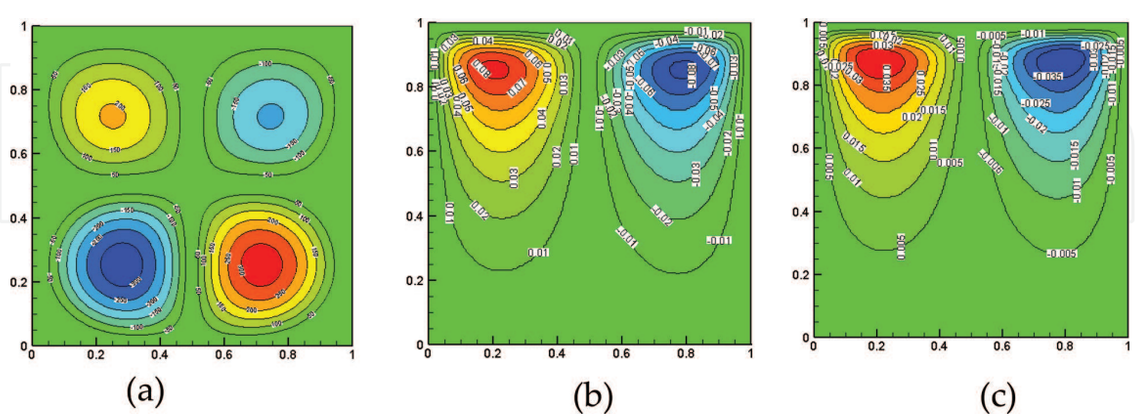

Figure 7.
Comparison of the steady state fluid velocity streamlines at Ra =10^5 and Pr = 0.025 for different Ha numbers in the case of linearly heated side walls.

Ra = 10^5. Numerical results in terms of flow and thermic structure show that the flow within the cavity takes place owing to the thermic buoyancy effects caused by the linearly heated walls, which is represented by the Ra number. The finding of Ra = 10^5 in the absence of magnetic field show that the flow is characterized by a multi-cellular behavior in which the re-circulating eddies or cells of relatively high

velocity are formed within the enclosure. The main awareness is about the cells that occur at upper left and lower right side which are circulating in the anti-clockwise direction and the rest are circulating in the clockwise direction (see **Figure 7a**). Near the adiabatic wall of the cavity, stronger cells are formed. Provided that we implement the same boundary conditions for the left (west) and right (east) walls of the enclosure, the two pairs of cells close to each of the linearly heated walls are symmetric. As forecasted, because of the boundary layer effects, the temperature field is sketched by sharp drop in its value near the adiabatic wall of the enclosure while it increases away from it in order to reach its maximum at the bottom boundary. Besides, we highlight that the temperature contour maps are not horizontally uniform in the core region of the cavity. We infer that an in-plane magnetic field has the tendency to slow down the movement of the fluid in the confined enclosure. As an outcome, the recirculating cells stretch or elongated in the rising vertical direction. In addition, the same process remains as Ha number increases provided the lower cells merge with the primary recirculating eddies which are at the outset positioned near the upper wall for Ha = 50 and 100 (**Figures 6** and 7). Furthermore, vertical stretching of the cells occurs in such a way that the eyes of the cells get closer to the upper boundary. As a result, a significant reduction in the fluid movement in the cavity is spotted. Beyond, the braking effect of the magnetic field is discerned from the depicted circulation. When steady states are reached, temperature stratification becomes ruling as the strength of the magnetic field increases and temperature contour maps become more horizontally uniform in the core region of the cavity. The observed dynamic and thermic behavior converge on a quasi-conduction regime and this vanquish the overall heat transfer in the cavity. The observed dynamic behavior is very useful and effective in the metals semiconductor crystal growth industries [35] and in controlling melts (**Figures 6** and 7).

To the author's knowledge, studies have thus far addressed a mesoscopic approach in an MHD open cavity with linearly heated wall (**Figure 1**). The objective of the present chapter is therefore to predict dynamic and thermic heat transfer in a crucial engineering application. In this section, the cavity is investigated at the high Ra number of 10^5, high Ha number (Ha = 50) and Pr number of 0.025. The exit section of flow on the open boundary moves downward and the movement of the flow gets limited with the increment of Ha number that it influences heat transfer from the linearly heated wall to the cold open boundary (see **Figure 8**). The effect

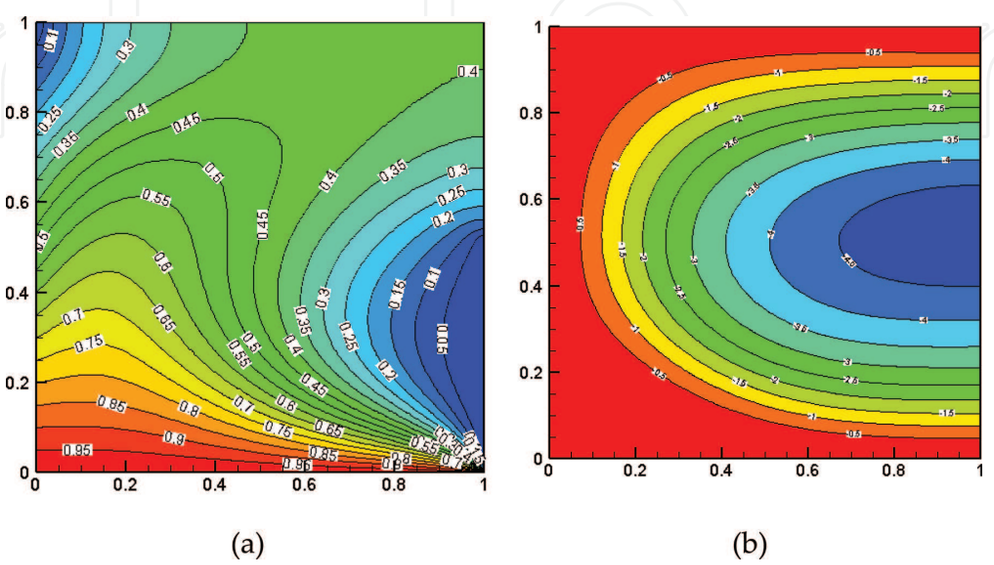

Figure 8.
Steady state fluid velocity streamlines (a) and isotherms (b) at Ha = 50, Pr = 0.025 and Ra = 10^5 for linearly heated open cavity.

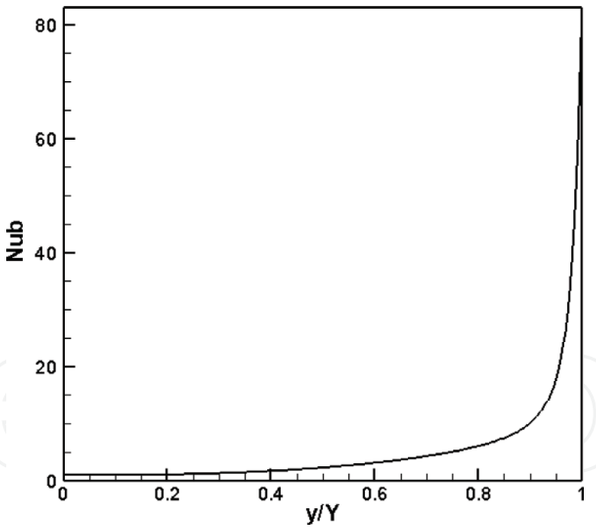

Figure 9.
Variation of local Nusselt number with distance at bottom wall in the case of linearly heated side wall for a MHD open cavity (Pr = 0.025, Ha = 50 and Ra = 10^5).

of the presence of the magnetic field is clear since the isotherms recede from the linearly heated left wall slowly and their gradient on the left wall declines extremely which it exposes the decrease in heat transfer in the open cavity. **Figure 9** illustrates the variation of local Nusselt number with distance at bottom wall in the case of linearly heated side wall for a MHD open cavity.

4. Conclusions

The present study considered steady state, laminar, two-dimensional MHD free convection within a liquid gallium filled square enclosure in the presence of in-plane magnetic field for different thermic boundary conditions. Lattice Boltzmann Method is utilized for simulation of this problem. The results of this method are validated in good agreement with previous numerical investigations. This investigation demonstrated ability of LBM for simulation of different boundary conditions at various elements affecting the stream. In addition this method helps to obtain stream function and isotherm counters smoothly. The governing equations are developed and solved by the LBM in the cases of linearly heated side walls and linearly heated left wall with cooled open right wall. In both cases, the upper wall of the enclosure is kept insulated. It was found that for the case of linearly heated side walls, a multi-cellular symmetric streamline behaviour was obtained for transverse applied magnetic fields. However, for the case of linearly heated left wall with cooled right wall, a two-cell (one primary and one secondary) feature was obtained. In general, the application of the magnetic field reduces the convective heat transfer rate in the cavity. Besides, the local Nusselt number at the bottom wall of the cavity exhibited oscillatory behavior along the horizontal distance for the case of linearly heated side walls whereas it increased continuously for the case of linearly heated left wall and cooled open right wall.

Nomenclature

C	lattice speed
c_i	discrete particle speeds
c_p	specific heat at constant pressure

F	external forces
f^{eq}	equilibrium density distribution functions
g^{eq}	equilibrium internal energy distribution functions
g	gravity
G	Buoyancy per unit mass
H	enclosure height
Ma	Mach number
Nu	Nusselt number
Pr	Prandtl number
Ra	Rayleigh number
T	temperature
x,y	cartesian coordinates
X	horizontal length of the cavity
Y	vertical length of the cavity
Ha	Hartmann number

Greek letters

ω_i	weighted factor indirection i
β	thermal expansion coefficient
τ	relaxation time
ν	kinematic viscosity
Δt	time increment
α	thermal diffusivity

Subscripts

av	average
H	hot
C	cold
b	bottom

Author details

Raoudha Chaabane[1,2]

1 Laboratory of Thermal and Energetic Systems Studies (LESTE) at the National School of Engineering of Monastir, University of Monastir, Tunisia

2 Preparatory Institute of Engineering Studies of Monastir (IPEIM), University of Monastir, Tunisia

*Address all correspondence to: raoudhach@gmail.com

References

[1] Mohamad AA. Natural convection in open cavities and slots, numer. Heat Transfer Part A. 1995;**27**:705-716

[2] Polat O, Bilgen E. Laminar natural convection in inclined open shallow cavities. International Journal of Thermal Sciences. 2002;**41**:360-368

[3] Mohamad AA, El-Ganaoui M, Bennacer R. Lattice Boltzmann simulation of natural convection in an open ended cavity. International Journal of Thermal Sciences. 2009;**48**:1870-1875

[4] Mohamad AA, Bennacer R, El-Ganaoui M. Double dispersion natural convection in an open end cavity simulation via lattice Boltzmann method. International Journal of Thermal Sciences. 2010;**49**: 1944-1953

[5] Kennedy P, Zheng R. Flow Analysis of Injection Molds. Munich: Hanser; 2013

[6] Fidaros D, Grecos A, Vlachos N. Development of numerical tool for 3D MHD natural convection. Annex XX. pp. 73-74

[7] Sathiyamoorthy M, Chamkha A. Effect of magnetic field on natural convection flow in a liquid gallium filled square cavity for linearly heated side wall(s). International Journal of Thermal Sciences. 2010;**49**:1856-1865

[8] Alchaar S, Vasseur P, Bilgen E. Natural convection heat transfer in a rectangular enclosure with a transverse magnetic field. Journal of Heat Transfer. 1995;**117**:668-673

[9] Garandet J, Alboussiere T, Moreau R. Buoyancy drive convection in a rectangular enclosure with a transverse magnetic field. International Journal of Heat and Mass Transfer. 1992;**35**: 741-748

[10] Rudraiah N, Barron R, Venkatachalappa M, Subbaraya C. Effect of a magnetic field on free convection in a rectangular enclosure. International Journal of Engineering Science. 1995;**33**:1075-1084

[11] Cowley M. Natural convection in rectangular enclosures of arbitrary orientation with magnetic field vertical. Magnetohydrodynamics. 1996;**32**: 390-398

[12] Teamah M. Hydro-magnetic double-diffusive natural convection in a rectangular enclosure with imposing an inner heat source or sink. Alexandria Engineering Journal. 2006;**45**(4): 401-415

[13] Ozoe H, Okada K. The effect of the direction of the external magnetic field on the three-dimensional natural convection in a cubic enclosure. International Journal of Heat and Mass Transfer. 1989;**32**:1939-1953

[14] Ece M, Buyuk E. Natural convection flow under a magnetic field in an inclined rectangular enclosure heated and cooled on adjacent walls. Fluid Dynamics Research. 2006;**38**(5): 546-590

[15] Al-Najem N, Khanafer K, El-Refaee M. Numerical study of laminar natural convection in tilted enclosure with transverse magnetic field. International Journal of Numerical Methods for Heat and Fluid Flow. 1998;**8**:651-672

[16] Jalil J, Al-Taey K. MHD turbulent natural convection in a liquid metal filed square enclosure. Emirates Journal for Engineering Research. 2007;**12**(2):31-40

[17] Gelfgat A, Bar-Yoseph P. The effect of an external magnetic field on oscillatory instability of convective flows in a rectangular cavity. Physics of Fluids. 2001;**13**(8):2269-2278

[18] Aleksandrova S, Molokov S. Three-dimensional buoyant convection in a rectangular cavity with differentially heated walls in a strong magnetic field. Fluid Dynamics Research. 2004;**35**: 37-66

[19] Kahveci K, Oztuna S. MHD natural convection flow and heat transfer in a laterally heated partitioned enclosure. European Journal of Mechanics—B/ Fluids. 2009;**28**:744-752

[20] Kefayati GHR, Gorji M, Ganji DD, Sajjadi H. Investigation of Prandtl number effect on natural convection MHD in an open cavity by Lattice Boltzmann Method. Engineering Computations. 2013;**30**:97-116

[21] Bilgen E, Yedder RB. Natural convection in enclosure with heating and cooling by sinusoidal temperature profiles on one side. International Journal of Heat and Mass Transfer. 2007;**50**:139-150

[22] Sarris IE, Lekakis I, Vlachos NS. Natural convection in a 2D enclosure with sinusoidal upper wall temperature, numer. Heat Transfer Part A. 2002;**42**: 513-530

[23] Varol Y, Oztop HF, Pop I. Numerical analysis of natural convection for a porous rectangular enclosure with sinusoidally varying temperature profile on the bottom wall. International Communications in Heat and Mass Transfer. 2008;**35**: 56-64

[24] Saeid NH, Yaacob Y. Natural convection in a square cavity with spatial side wall temperature variation, numer. Heat Transfer Part A. 2006;**49**: 683-697

[25] Martinez D, Chen S, Matthaeus W. lattice Boltzmann magneto hydrodynamics. Physics of Plasmas. 1994;**6**:1850-1867

[26] Chaabane R, Askri F, Nasrallah SB. Parametric study of simultaneous transient conduction and radiation in a two-dimensional participating medium. Communications in Nonlinear Science and Numerical Simulation. 2011;**16**(10): 4006-4020

[27] Saha LK, Hossain MA, Gorla RSR. Effect of Hall current on the MHD laminar natural convection flow from a vertical permeable flat plate with uniform surface temperature. International Journal of Thermal Science. 2007;**46**:790-801

[28] Chaabane R, Askri F, Nasrallah SB. Analysis of two-dimensional transient conduction-radiation problems in an anisotropically scattering participating enclosure using the lattice Boltzmann method and the control volume finite element method. Journal of Somputer Physics Communications. 2011;**182**(7): 1402-1413

[29] Lamsaadi M, Naimi M, Hasnaoui M, Mamou M. Natural convection in a vertical rectangular cavity filled with a non-Newtonian power law fluid and subjected to a horizontal temperature gradient. Numerical Heat Transfer, Part A: Applications. 2006;**49**:969-990

[30] Chaabane R, Askri F, Nasrallah SB. Application of the lattice Boltzmann method to transient conduction and radiation heat transfer in cylindrical media. Journal of Quantitative Spectroscopy and Radiative Transfer. 2011;**112**(12):2013-2027

[31] Chaabane R, Askri F, Jemni A, Nasrallah SB. Numerical study of transient convection with volumetric radiation using an hybrid lattice Boltzmann BGK-control volume finite element method. Journal of Heat Transfer. 2017;**139**(9):092701

[32] Raoudha C, Askri F, Jemni A, Nasrallah SB. Analysis of Rayleigh-Bénard convection with thermal

volumetric radiation using lattice Boltzmann formulation. Journal of Thermal Science and Technology. 2017; **12**(2):JTST002. https://www.jstage.jst.go.jp/browse/jtst/12/0/_contents/-char/en0

[33] Mohamad AA. Applied Lattice Boltzmann Method for Transport Phenomena, Momentum, Heat and Mass Transfer. Calgary: Sure; 2007

[34] Succi S. The Lattice Boltzmann Equation for Fluid Dynamics and beyond, Clarendon Press. Oxford: London; 2001

[35] Series RW, Hurle DTJ. The use of magnetic fields in semiconductor crystal growth. Journal of Crystal Growth. 1991;**133**:305-328